Synthesis and adsorption capacity of biochar derived from *Tamarindus indica* shell for the removal of heavy metal

Rajakumar S.[1]*, Hemavathi S.[2], El-marghany A.[3] and Warad I.[4,5]

[1]Department of Civil Engineering, University VOC College of Engineering, Anna University Thoothukudi Campus, Thoothukudi–628 008, Tamil Nadu, India

[2]Department of Civil Engineering, K. Ramakrishnan College of Technology, Trichy–621 112, Tamil Nadu, India

[3]Department of Chemistry, College of Science, King Saud University, P.O. Box 2455, Riyadh 11451, Saudi Arabia

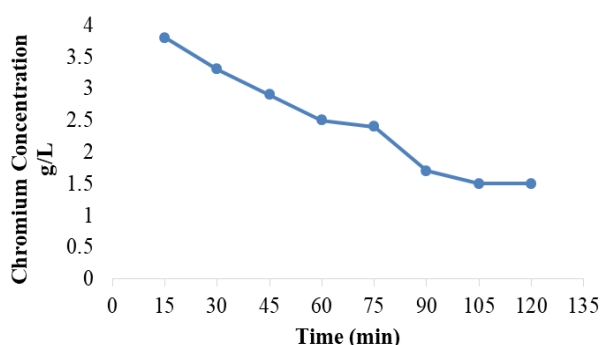[4]Department of Chemistry, AN-Najah National University, P.O. Box 7, Nablus, Palestine

[5]Research Centre, Manchester Salt & Catalysis, Unit C., 88-90 Chorlton Rd, M15 4AN Manchester, United Kingdom

*to whom all correspondence should be addressed: e-mail: civilrajas@gmail.com

Graphical abstract

Abstract

Tamarindus indica shell biochar is employed as an alternate adsorbent precursor for the removal of heavy metal ions from aqueous solutions. It investigated the Tamarindus indica shell biochar's capacity to absorb chromium (Cr), copper (Cu), and Lead (Pb). This study showed the extensive explored how biosorption experimental limitations counting primary metal attentiveness, adsorbent dosage, temperature, and contact time affect the process. The complete analysis of the Tamarindus indica shell's adsorption capability with respect to chromium, copper, and nickel removal was conducted using a batch adsorption procedure. Determining the amount of heavy metal removal in the aqueous solution proceeded by Gas Chromatography (GC). The experimental data analyzed using the Yoon Nelson and Thomson models to regulate the equilibrium isotherms. The optimal parameters for the overall adsorption model were determined by using ANOVA. Investigate the adsorbent's surface area to determine the presence of heavy metal presents using SEM, XRD, and FTIR techniques. Each researched heavy metal's adsorption capability is listed below: Cr = 6.07 mg/L, Cu = 5.53 mg/L and Pb = 5.497mg/L with a removal percentage of 64%, 92% and 78%, respectively. The results showed that biochar generated from Tamarindus indica shells is an effective adsorbent for removing copper from aqueous solutions but not a viable biosorbent for removing chromium. Also, the regenerated column's adsorption capability was examined. The outcomes of the research demonstrated that biochar, which pis producedfrom Tamarindus indica shell can be employed as an efficient and reasonably priced adsorbent to remove heavy metal ions from aqueous solutions.

Keywords: Heavy metal, biochar, adsorption, ANOVA analysis, kinetic study, regeneration

1. Introduction

Toxic metals called heavy metals are discrete metals and metal composites that have harmful effect in people's health. Because heavy metals can impair human health even at low concentrations in the environment, their presence in water streams, air, soil, and food has become problematic (Praveen *et al.*, 2021). One of the issues that people have is heavy metal pollution in the water heavy metal can be toxic to life. It poses a risk to the ecosystem, including to the health of people, animals, and plants. In order to manage the degree of water pollution, The Environmental Protection Agency (EPA) and the World Health Organization (WHO) have established the maximum permissible discharge level into ecosystems (Gokulan *et al.*, 2019). Because of population increase, rapid industrial and agricultural development, and a high concentration of harmful heavy metals in water sources, there is a threat to human health and natural systems. Exposure to heavy metals like lead (Pb), chromium (Cr), and copper (Cu) can cause heavy metal poisoning (Rao *et al.*, 2021). When heavy metals bind to specific cell components, organs cannot function properly. The effects of heavy metal poisoning can be irreversible and life-threatening. Most heavy metals are absorbed, stored, and even accumulate in the human body, causing persistent problems (Sujatha *et*

al., 2021). Hence, before releasing waste aqueous solution into the environment, these heavy metals from industrial influents must be removed. A critical issue is the removal of such hazardous metal ions from aqueous solutions (Ravindiran *et al.*, 2019). A variety of methods have been used to remove heavy metal ions from aqueous solutions, including chemical precipitation, ion-exchange, adsorption, membrane filtration, electrochemical treatment methods, and so on (Kalyani *et al.*, 2021). One of the most significant physico-chemical treatment methods for removing heavy metals from aqueous solutions is adsorption. The natural availability of biomaterials in the environment and their inexpensive cost makes using biochar, which is made from them, quite popular (Gokulan *et al.*, 2019). Several attempts have been undertaken to adsorb heavy metals from aqueous solutions using the least expensive and uncommon adsorbents, such as aquatic plants, plant wastes, agricultural and industrial by-products. The primary goal of this research is to use the adsorption technique to remove heavy metals like chromium (Cr), copper (Cu), and lead (Pb) (Gokulan *et al.*, 2022). Heavy metals were removed using biochar made from Tamarindus indica shells as an adsorbent. Although there have been many applications for biochar, they have not gotten significant consideration. Assessment of biochar as low-cost adsorbent for aqueous treatment should be painstaking (Mahendran *et al.*, 2021). As a result, biochar, a byproduct of the shell of Tamarindus indica, was used as a substitute adsorbent precursor in this work for the adsorption-based removal of heavy metal ions from aqueous solutions. After the adsorption procedure, the level of heavy metals in an aqueous solution is assessed using Gas chromatography (GC) (Ravindiran *et al.*, 2019). For the purpose of separating and analysing chemicals that can be vaporized without decomposing, it is an analytical chemistry technique. The experimental data was analyzed using the Yoon Nelson and Thomson models to establish the equilibrium isotherms (Gokulan *et al.*, 2021). The ANOVA analysis examined statistically significant variations between the means and the treatment variance. SEM, XRD, and FTIR techniques should be used to examine the adsorbent's surface area to detect the presence of heavy metals (Madhu *et al.*, 2021). The thorough analysis demonstrates the Tamarindus indica shell-derived biochar's adsorption potential.

2. Materials and methods

2.1. Biochar preparation

The biochar was made using a common leftover stalk of Tamarindus indica shell that was discovered as a pertinent feedstock. The stalks were collected from farmland (Gokulan *et al.*, 2019). Deionized water was used to wash the Tamarindus indica shell numerous times until the soil was removed. Using a multi-purpose swing grinder, a powdered sample (1mm) was created after 3–4 days of air drying (Priya *et al.*, 2020). Following that, each trial was carefully packed into a ceramic pot and sealed with a lid to produce an oxygen-limited environment for the heating process. Heating administered in a muffle furnace at a degree of $50^{o}C min^{-1}$ until a desired ultimate temperature

of 400 °C was reached, which was then sustained for 3 h (Gokulan *et al.*, 2021). The biochar product was powdered after it had naturally cooled enough that the entire sample could pass a 150-mesh sieve while still being reserved on a 100-mesh sieve (Murugadoss *et al.*, 2021). Fresh biochar trials of element size 60-100 mm were consequently attained.

2.2. Preparation of synthetic aqueous solution

To create stock solutions containing 1000 mg/L of metal ions, analytical grade CuSO4.5H2O, CrCl3.6H2O, and Pb metal were dissolved in distilled water. All the chemicals utilized were of the highest analytical quality (Gokulan *et al.*, 2022). The studies used distilled water exclusively. Prepared by dissolving 2.5 g of CuSO4.5H2O, 4.2 g of CrCl3.6H2O, and 1.5 g of Pb (metal) in 1000 mL of distilled water, stock solutions of 1000 mg/L for copper, chromium, and lead ions (Kumar *et al.*, 2021).

2.3. Adsorption study

Inner diameter of 3cm and 50cm length glass column used for adsorption study. Particle sizes of the biochar, which is made from the shell of the tamarind indica plant, range from 0.5 to 1.5 mm (Gokulan *et al.*, 2019). The column was filled with adsorbent, and the bottom was covered with glass wool. From literature survey the optimum height of 10 cm column used for this study (Pushpa *et al.*, 2021). The labor flow rates ranged from 2.0mL/min. At predefined intervals, the residual heavy metal content in the effluent samples was assessed. Column investigations ended when the column neared fatigue (Lo *et al.*, 2012). For practical reasons, the column studies are conducted at room temperature.

2.4. Gas chromatography (GC)

The water used for GC met the requirements of ISO Grade 78-2:1982, and the heavy metal copper, chromium and lead stock standard solutions were obtained (Gokulan *et al.*, 2021). Heavy metal solution from several sources was used for the method validation and calibration trials as well as an independent source for quality control (Sundar *et al.*, 2021). The gradient pump in the GC system had a flow rate of 0.50 mL/min., an auto sampler with a 10 µL injection loop, a column thermostat set at 27°C, an eluent generator supplying 40 ml/L, and a conductivity detector (Ravindiran *et al.*, 2014). The suppression column was a LCGC, and the column was a silicon-based column, both in 4mm format. Each sample ran for a total of 20 minutes (Senthil Kumar *et al.*, 2021). The working range, performance, and calibration data for a concentration decade looking at standard solutions of heavy metal concentrations were evaluated statistically.

2.5. Kinetic study

2.5.1. Yoon Nelson model for adsorption study

Due to the Yoon-Nelson Model's lack of a need for in-depth adsorbate understanding, it is easier (Gokulan *et al.*, 2013). According to this model, the likelihood of each adsorbate molecule adhering to the adsorbent decreases at a rate that is proportional to both the likelihood of adsorbate adsorption and the likelihood of adsorbate breakthrough

on the adsorbent (Rajeshkumar *et al.*, 2023). It is a model for a single component system, the linearized equation of model expressed as Eq:

$$In\frac{Ct}{Co-Ct} = kyt - \tau ky$$

The rate constant is kyt (min^{-1}), and (min) is the shortest period necessary for 50% adsorbate breakthrough. Yoon Nelson linear plots are used as a model. The intercept and slope of the linear plot of the ln [Ct/C0-Ct] vs. t graph can be used to determine the parameters ky.

2.5.2. Thomson model for adsorption study

By means of Thomson model, the association among internal then external progressions of adsorption found (Gokulan *et al.*, 2018). The Thomson model described as

$$In\left(\frac{Co}{Ct}-1\right) = k_{TH}q_eW - k_{TH}C_ot$$

2.6. ANOVA analysis

Experiencing cumulative inconsistency originating from exclusive statistics established is separated from methodical elements and random factors using a statistical inquiry approach called analysis of variance (ANOVA) (Kumar *et al.*, 2017). It establishes how a dependent variable in a regression analysis is impacted by an independent unknown. A one-way ANOVA is used in this study to analyze the connection between the dependent and independent variables. To assess the impact of persuasive parameters on response, the ANOVA method has frequently been used (Gokulan. and Kumar, 2014). This is frequently done through cross authentication, testing, and estimation. The underpinning for scheming taxing is completed exclusively of testing model (Krishna *et al.*, 2015). Yet, this is frequently not practicable in corporeal science because there are frequently not enough examples (Ravindiran. and Ragunath, 2014). Then, A more effective method is used, which repeatedly removes items from the data collection to do caricature forecast testing.

$$F = \frac{MST}{MSE}$$

Where:

F = ANOVA coefficient

MST = Mean sum of squares due to treatment

MSE = Mean sum of squares due to error

Experimental data should be analyzed using a second-order polynomial model to increase the unpredictability in the progression of coagulation and flocculation. A design expert also established the analysis of the change.

2.7. Characterization study

2.7.1. SEM analysis
The material and particle size distribution were graphically described using scanning electron microscope (SEM) equipment. The Shimadzu SD analyzer performed the SEM test (Praveen *et al.*, 2021). Using a PerkinElmer ZSD3500 analyzer, a thermogravimetric analysis was done to calculate the sample mass as a function of temperature and constant heating rate.

2.7.2. XRD study
Using the X-ray diffraction (XRD) method and an ARL EQUINOX 9900 XRD with V X-ray diffractometer outfitted with monochromatized Cu K radiation (1.4258), the crystal structure and phase purity were determined (Saravanan *et al.*, 2022). Energy dispersive X-ray spectroscopy was performed using a Phoneix instrument X-Max energy dispersive X-ray spectrometer. Cu2O SPs' morphology was evaluated using a field emission scanning electron microscope (Ravindiran, 2014). On an XPS spectrometer, X-ray photoelectron spectroscopy (XPS) was conducted.

2.7.3. FTIR analysis
Fourier transform infrared spectroscopy was used to identify the surface species (FT-IR). A Shimadzu-450 spectrometer was used to capture the FT-IR spectra in Cu pellets. Copper was added to the samples after which they were dehydrated at 150 °C and exposed to ultraviolet bright (Jankowska *et al.*, 2022). The capsules were tested instantly after processing under natural illumination in the mid-infrared spectrum.

2.8. Regeneration of adsorbent
By electrically heating the adsorbent to 280°C in both an inert and an environment with air, thermal regeneration was accomplished (Jegan *et al.*, 2020). The adsorbent was heated to between 300°c and 500°c in a muffle furnace during the hot water extraction process, twice washed with DI water and an HCL solution, and then dried for an additional two hours in a hot air oven (Gokulan *et al.*, 2020). The effectiveness of the regenerated adsorbent's regeneration was determined by measuring the heavy metal removal capacity.
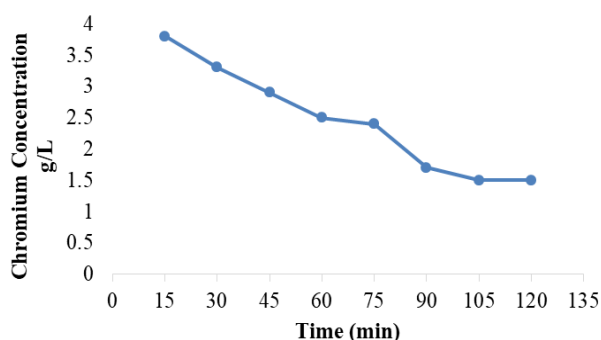
3. Result and discussion
3.1. Adsorption study
3.1.1. Chromium adsorption (Cr)
Batch adsorption research was conducted to ascertain the amount of chromium removed. The chromium (Cr) concentration range of 4.2 g/L was employed for the adsorption research as a reference value (Ilavarasan *et al.*, 2022). 10 cm was chosen as the ideal height for the experimental investigation. The Tamarindus indica shell-derived biochar was placed in a class column with 0.5 mL/min exit ranges. The initial treatment efficiency started at 15 minutes in the 3.8 g/L level. After increasing it for the next 15 minutes, the column's removal efficiency reached 1.5 g/L after 105 minutes (Jegan *et al.*, 2020). As shown in Table 1 and Figure 1, the column reached saturation under these circumstances after 120 minutes.

Table 1. Chromium removal

| Time (Min)	Chromium Concentration g/L
15	3.8
30	3.3
45	2.9
60	2.5
75	2.4
90	1.7
105	1.5
120	1.5

Figure 1. Chromium removal

3.1.2. Copper Adsorption (Cu):

Batch adsorption research was conducted to ascertain the amount of copper removed. The copper (Cu) concentration of 2.5 g/L or less was selected as the reference level for the adsorption experiment (Hariharan *et al*., 2022). It was determined that 10 cm was the ideal height for the experimental investigation. After being filled with biochar made from Tamarindus indica shells and having exit ranges of 0.46 mL/min, the column reached saturation after 105 minutes, as shown in Table 2 and Figure 2.

Table 2. Copper removal

| Time (Min)	Copper Concentration g/L
	g/L
15	2.4
30	2.0
45	1.6
60	1.2
75	0.75
90	0.20
105	0.20
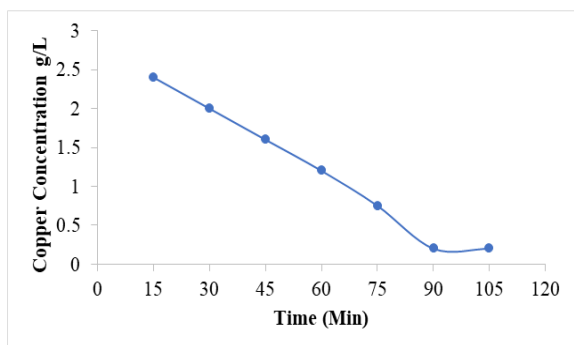
Figure 2. Copper removal

3.1.3. Lead Adsorption (Pb)

To ascertain the Lead elimination by adsorption investigation, a batch adsorption study was conducted. Lead (Pb) concentrations between 1.5 g/L were selected as a starting point for the adsorption experiment (Kalyani *et al*., 2020). During the experimental investigation, a height of 10 cm was determined to be ideal. The Tamarindus indica shell-derived biochar was placed in a class column with exit ranges of 0.45 mL/min. The initial treatment efficiency started at 15 minutes in the 1.4 g/L level. In the following 15 minutes, the removal efficiency increased, and after 75 minutes, the column's removal efficiency was 0.33 g/L (Praveen *et al*., 2022). Under this condition, the column became saturated after 90 minutes, as shown in Table 3 and Figure 3.

Table 3. Lead removal

Time (Min)	Lead Concentration g/L
	g/L
15	1.4
30	1.1
45	0.98
60	0.72
75	0.33
90	0.33
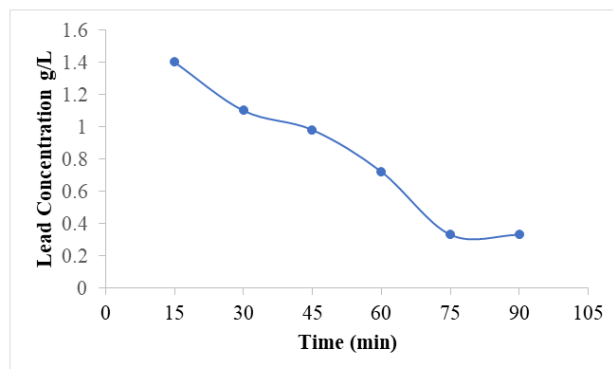
Figure 3. Lead removal

3.1.4. Heavy metal adsorption

The heavy metals (Cr, Ca, and Pb) used in this extensive adsorption investigation were taken in the range of 4.2g/L, 2.5g/L, and 1.5g/L. In accordance with the literature, the ideal column height was determined to be 10 cm. Gas chromatography (GC) was used to analyze the amount of heavy metal elimination every 15 minutes (Sujatha *et al*., 2021). Initial treatment efficiency in the analysis of chromium adsorption started at 15 minutes in the 3.8 g/L level. After being increased for the following 15 minutes, the column's removal efficiency reached 1.5 g/L in 105

minutes, and in 120 minutes the column reached saturation. Chromium was removed from the biochar made from Tamarindus indica shells at a 64% removal rate (Praveen *et al.*, 2021). The initial treatment efficiency started at 15 minutes in the 2.4 g/L level in the subsequent experiment about copper removal at a concentration of 2.5 g/L. In the following 15 minutes, the removal efficiency rose, and after 90 minutes, the column's removal efficiency was 0.20 g/L with a 92% removal rate. The third lead elimination study went forward with a concentration of 1.5 g/L. In the following 15 minutes, the removal efficiency rose, and after 75 minutes, the column's removal efficiency was 0.33 g/L with a 78% removal rate (Jegan *et al.*, 2020). This thorough study demonstrated that the biochar made from Tamarindus indica shells, with an adsorption column height of 10 cm, was effective at removing copper with a 92% removal rate.

3.2. Gas chromatographic study

The samples were taken after the adsorption research and put in vials that were maintained in the fridge in order to analyze the chromatogram. A 10 µl sample was taken from the intake region and passed through the mobile phase and stationary phase (Pushpa *et al.*, 2019). The perfect heavy metal level determined by using graph of GC result. In order to assess graphical representation, Class VP Software and GC was hired to establish the quantity of heavy metals (Ali *et al.*, 2021). The peak's height and area in the graphical representation were used to determine the sample's heavy metal concentration (Figure 4).
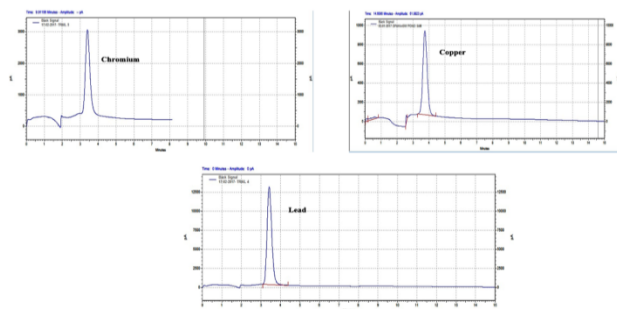

Figure 4. Heavy metal (Cr, Cu & Pb) analysis by Gas Chromatography (GC)

3.3. Yoon Nelson model for adsorption study

According to results, heavy metal removal exhibited a stronger adsorption break through with a copper $R2$ value larger than 0.9835, lead $R2$ value 0.9101, and chromium $R2$ value 0.8754 (Jegan *et al.*, 2021). In the row of heavy metals, the rate constants were 4.51; 5.20; and 4.93. Heavy metals have $Ky(min^{-1})$ values of 0.474, 0.624, and 0.551. This meant that the kinetic values of heavy metal removal were mostly responsible for the experimental outcomes.
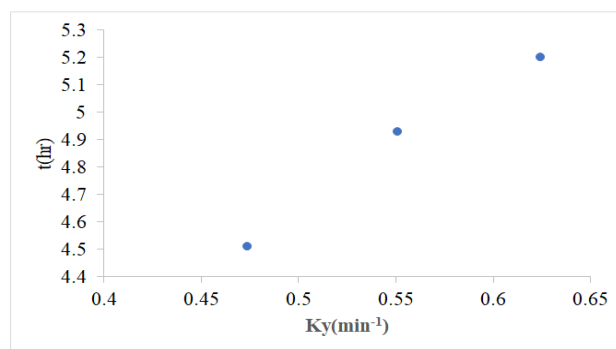

Figure 5. Heavy metal removal by Yoon – Nelson model

3.4. Thomson model for adsorption study

The elimination of heavy metals through adsorption was analyzed using the Thomson model. The projected breakthrough curve and the measured adsorption process agreed. The mass (m), concentration time (t), and copper metal's regression coefficient ($R2$) of 0.9817 all affect the value of kt (Kumar *et al.*, 2022). As seen by the lowest kt value at highest Co, the adsorption kinetics supported at the highest adsorbate concentration. The initial kt values increased to 0.9104 for copper, 0.7159 for chromium, and 0.8273 for lead from lower levels. According to Table 4 and Figure 5, Copper, Chrome, and Lead equilibrium uptake capacities (qo), which were 73.50, 27.35, and 41.72 respectively, were somewhat increased (Ragunath *et al.*, 2022). The decline in qo demonstrated that there is an inverse correlation between bed height, contact time, and adsorption capacity (Tables 5 and 6).

Table 4. Heavy metal removal by Yoon – Nelson model

Materials	$Ky(min^{-1})$	$\tau(hr)$	R^2
Chromium	0.474	4.51	0.8754
Copper	0.624	5.20	0.9835
Lead	0.551	4.93	0.9101

Table 5. Thomson model for heavy metal removal

Heavy metal	$k_t \times 10^{-3}$ (mL/(min.mg)	q_o (mg/g)	R^2
Chromium (Cr)	0.7159	27.35	0.9642
Copper (Ca)	0.9104	73.50	0.9817
Lead (Pb)	0.8273	41.72	0.9635

3.5. ANOVA for Quadratic model

The Model F-value of 725.64 suggests that the model is significant. Just 0.2% of the time may noise be the cause of an F-value this high. In cases when the P-value is fewer than 0.0600, archetypal relations are considered important

(DadbanShahamat *et al.*, 2022). If the value is more than 0.0001, then the model relations are not substantial. If there are many extraneous terms, model reduction might improve this model. The F-value of 0.6532 for dearth of suitability shows that the absence of appropriateness is not

significantly different from the pure error (Wang *et al.*, 2021). The unintentional likelihood of noise causing a significant Lack of Fit F-value is 92.56% (Figure 6).
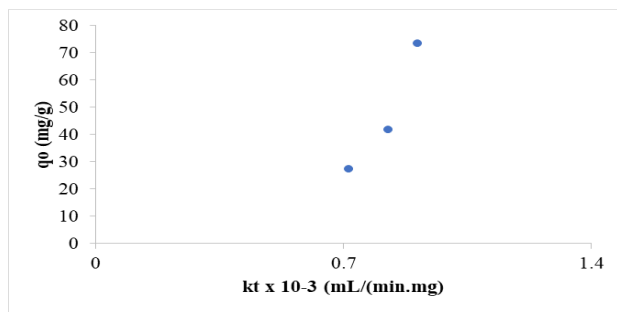

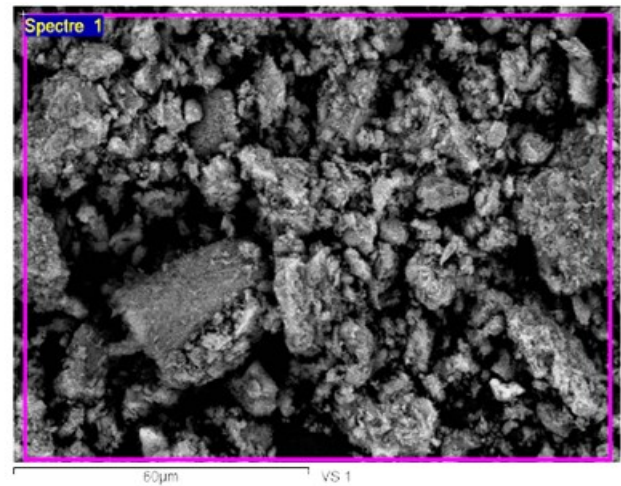
Figure 6. Thomson model for heavy metal removal

Figure 7. SEM analysis of Biochar adsorbent

Table 6. ANOVA for Quadratic model

Source	Sum of Squares	df	Mean Square	F-value	p-value	Remarks
Model	481.62	19	48.27	725.64	< 0.0001	Significant
A-Initial Concentration	297.41	1	256.74	5471.77	< 0.0001	
B-PH Solution	197.52	1	104.56	1755.15	< 0.0001	
C-Contact Time	44.56	1	27.45	384.78	< 0.0001	
D-Adsorbent Dosage	84.31	1	88.12	1378.16	< 0.0001	
AB	0.9415	1	0.8417	9.84	0.0032	
AC	3.21	1	3.56	38.73	< 0.0001	
AD	3.74	1	3.20	41.97	< 0.0001	
BC	4.59	1	4.12	50.85	< 0.0001	
BD	0.2411	1	0.1048	1.75	0.2124	
CD	2.73	1	2.77	34.11	< 0.0001	
A²	58.44	1	56.82	681.55	< 0.0001	
B²	31.24	1	31.22	285.97	< 0.0001	
C²	38.77	1	29.47	354.42	< 0.0001	
D²	9.32	1	11.53	163.47	< 0.0001	
Residual	2.99	13	0.0714			
Deficit of Fit	1.6532	12	1.0497	1.2497	1.9576	not significant
Absolute Error	1.6487	9	1.1754			
Core Total	751.72	28				

3.6. Characterization of Biochar adsorbent

3.6.1. SEM analysis of Biochar adsorbent

Figure 7 shows the SEM images of the adsorbent; the wolfram deposit and diatomite-based ceramic have a shape that is nearly spherical and a rough, porous surface. From the inside to the exterior of ceramicite, there are numerous pores (Moradi *et al.*, 2022). Thus, the surface and internal structure of ceramsite is likely to experience Cu2+ ion adsorption in solution. The porous structural nature received a dump of the ca2+ adsorbent that was already present in the surface area. The Pb component was supported by the adsorbent's surface-level structure (Lach *et al.*, 2022). Optimizing the circumstances for getting heavy metal particle dispersions to apply to a fibrous carrier was the challenge. As crosslinking bridges, heavy metals were used to create adsorbent nanoparticles (Haris *et al.*, 2022). The molar ratio is the primary determinant of the process parameters for a given constant concentration of heavy metal in mixtures, and the properties of the particles indicate the presence of heavy metal in the adsorbent.

3.6.2. XRD analysis of Biochar adsorbent

The typical XRD pattern of the Cu, Cr, and Pb sample is displayed in Figure 8. All the deflection crests of the heavy metal sample were in upright contract with the cubic phase of the heavy metal, which had a framed relentless of 5.7145 nm (Zhu *et al.*, 2023). The replications of hydroplanes of cubic heavy metals were thought to be responsible for the peaks at 3 values of 33.75°, 28.52°, 30.13°, 56.84°, and 64.82°. There were also found to be other impurities, like metal Cu, Cr, and Pb (Cheng *et al.*, 2023). The heavy metals sample's good crystallinity was shown by the strong and precise diffraction peaks. The EDS analysis revealed that the copper to oxygen atom ratio was nearly 3:2, which supported the hypothesis that the synthesized sample included the heavy metal.
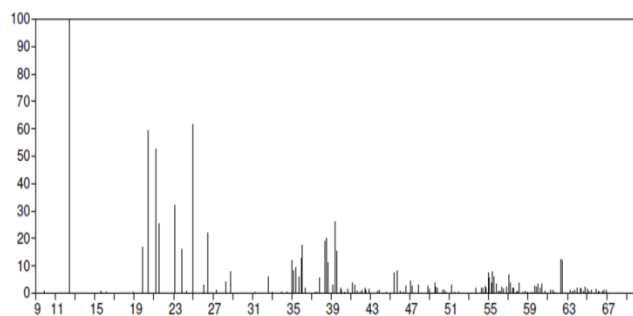
Figure 8. XRD analysis of Biochar adsorbent

3.6.3. FTIR analysis of Biochar adsorbent

Figure 9 showed the FTIR spectra of the heavy metal adsorbent. The modest absorption peaks at 5841 and 3574/cm, respectively, represent the stretching and bending vibrations of the OH- bond, demonstrating the simultaneous existence of coordinated water and a few adsorbed water (Bumajdad . and Hasila, 2023). The peak at 1682 cm for the adsorbent in Figure 9 might be attributed to C-H flexural vibration, whereas the bands at 1678 cm and 1578 cm are attributed to O-H deformation vibration and C=C stretching vibration, respectively. The carboxyl groups' (-C=O-) and C-H bending vibrations, respectively, are responsible for the large absorption peaks at 1547 cm and 745 cm, respectively (Ru *et al*., 2021). The wide band seen between 1384 and 1012 cm is caused by vibrations that stretch the C-O bond and bend the O-H bond (in plane).
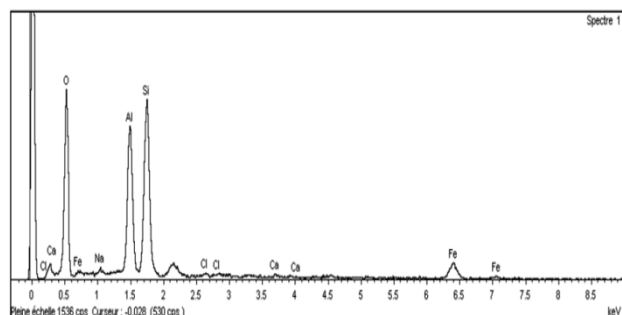

Figure 9. FTIR analysis of Biochar adsorbent

3.7. Column regeneration study

In order to evaluate the adsorbent's reusability, the cleaned column was utilized once more for the ensuing adsorption cycle, which was followed by four further adsorption cycles. To test for reusability, the adsorbent was repackaged and used fresh once more (Charazinska *et al*., 2021). corresponding to three study cycles. The effectiveness of heavy metal removal decreased after the first four cycles.

4. Conclusion

In this study, a low-cost alternative adsorbent for the removal of the ions Chromium (Cr), Copper (Cu), and Lead (Pb) from aqueous solution was examined. The biochar was made from the shell of the Tamarindus indica plant. For the elimination of chromium (Cr), copper (Cu), and lead (Pb), the ideal adsorption conditions were identified as a function of pH, adsorbent dosage, initial metal ion concentration, and solution contact duration. According to the study, the following is a list of heavy metals' adsorption

capacities: With elimination percentages of 64%, 92%, and 78%, respectively, Cr, Cu, and Pb are at 6.07 mg/L, 5.53 mg/L, and 5.497 mg/L, respectively. The findings demonstrated that biochar made from Tamarindus indica shells is not a viable biosorbent for chromium elimination but performs well as an adsorbent to extract copper from liquid samples. Kinetic analysis of the adsorption capability of biochar material against heavy metal was well calculated with R^2 = 0.9817, according to the Yoon Nelson and Thomson models. The surface alteration caused by heavy metal adsorption in the adsorbent is seen in the SEM, XRD, and FTIR characteristics. The regenerative capability of the adsorbent in contradiction of heavy metal adsorption studied. According to this thorough study's findings, Tamarindus indica shell biochar seems to be a reliable, affordable, and for exclusion of heavy metals from liquid samples, use a replacement sorbent pioneer.

5. Conflict of Interest

The authors declare no conflict of interest.

References

Ali A.A., Ouda M., Naddeo V., Puig S and Hasan W.S. (2021). Integrated electrochemical-adsorption process for the removal of trace heavy metals from wastewater, Case studies in *chemical and environmental engineering*, **4**, ID. 100147.

Bumajdad A and Hasila P. (2023). Surface modification of date palm activated carbonaceous materials for heavy metal removal and CO2 adsorption, *Arabian journal of chemistry*, **16**, ID. 104403.

Charazinska S., Lochynski P and Burszta-Adamiak E. (2021). Removal of heavy metal ions form acidic electrolyte for stainless steel electropolishing via adsorption using Polish peats, *Journal of water process engineering*, **42**, ID. 102169.

Cheng Y., Li M and Song Y. (2023). Theoretical study of M2CO2 MXenes stability and adsorption properties for heavy metals ions removal from water, *Computational material science*, **220**, ID. 112042.

DadbanShahamat Y., Masihpour M., Borghei P and Rahmati H.S. (2022). Removal of azo red-60 dye by advanced oxidation process O3/UV from textile wastewaters using Box-Behnken design, *Inorganic chemistry communications*, **143**, 109785.

Gokulan R and Kumar N.M. (2014). Optimization of Conditions for Bio hydrogen Production from Industrial Waste by Anaerobic Co-digestion, *Nature Environment and Pollution Technology*, **13** (04), 791–794.

Gokulan R., Avinash A., Prabhu G.G and Jegan J. (2019). Remediation of remazol dyes by biochar derived from Caulerpa Scalpelliformis - An eco-friendly approach, *Journal of Environmental Chemical Engineering*, **7**(5), 103297.

Gokulan R., Balaji S and Sivaprakasam P. (2021). Optimization of Remazol Black B Removal Using Biochar Produced from Caulerpa scalpelliformis Using Response Surface Methodology, *Advance in Materials sciences and Engineering*.

Gokulan R., Kalyani G and Killi S. (2022). Experimental Investigation on Reactive Orange 16 Removal Using Waste

Biomass of Ulva prolifera, *Advances in material sciences and engineering*, Article ID 2689385.

Gokulan R., Kalyani G and Killi S. (2022). Removal of Reactive Red 120 in a Batch Technique Using Seaweed-Based Biochar: A Response Surface Methodology Approach, *Journal of Nanomaterials*, Hindawi Publications, Article ID 7604383.

Gokulan R., Prabhu G.G and Jegan J. (2019). A novel sorbent Ulva lactuca-derived biochar for remediation Remazol brilliant orange 3R in packed column, *Water Environment Research*, **91**(7), 642–649.

Gokulan R., Prabhu G.G and Jegan J. (2019). Remediation of complex remazol effluent using biochar derived from green seaweed biomass, *International Journal of Phytoremediation*, **21**(12), 1179–1189.

Gokulan R., Prabhu G.G., Avinash A and Jegan J. (2020). Experimental and Chemometric analysis of bioremediation of remazol dyes using biochar derived from green seaweeds, *Desalination and Water Treatment*, **184**, 340–353.

Gokulan R., Prabhu G.G., Murugadoss R.J and Hariharasuthan S. (2018). Optimization of bio-hydrogen production from bio-wastes, *Ecology, Environment and Conservation*, **24** (1), 284–287.

Gokulan R., Pradeepkumar S and Elias G. (2021). Continuous Sorption of Remazol Brilliant Orange 3R Using Caulerpa scalpelliformis Biochar, *Advances in Materials Science and Engineering*, Article ID 6397137, 7

Gokulan R., Praveen S., Avinash A and Saravanan S. (2021). Soft computing-based models and decolorization of Reactive Yellow 81 using Ulva Prolifera biochar, *Chemosphere*, **287**, Part 4, Jan 2022, 132368.

Gokulan R., Sathish N and Kumar R.P. (2013). Treatment of Grey Water Using Hydrocarbon Producing Botryococcus braunii, *International Journal of Chemtech Research*, **05**(03), 1390–1392.

Gokulan R., Vijayakumar A., Kumar V.R and Praveen S. (2020). Remazol Effluent Treatment in Batch and Packed Bed Column Using Biochar Derived from Marine Seaweeds, Nature, *Environment and Pollution Technology*, **19**, 1931–1936.

Gopala Krishna G.V.T., Sivasankar V. and Senthil Kumar M. (2015). Coagulation performance evaluation of natural and synthetic coagulants in wastewater treatment, *ARPN Journal of Engineering and Applied Sciences*, **10**(6).

Hariharan T., Gokulan. R., Saravanan R.V and Rahman D.Z. (2022). Batch and Packed Bed Column Studies of Azo Dyes Adsorption from the Aqueous Solutions Using Activated Sugarcane Bagasse Charcoal Adsorbent: Isotherm and Kinetic Studies, *Global NEST Journal*.

Haris M., Khan M., PazFerreiro J., Mahmood N and Eshtiagi N. (2022). Synthesis of functional hydrochar from olive waste for simultaneous removal of azo and non-azo dyes from water, *Chemical engineering journal advances*, **9**, 100233.

Ilavarasan N., Rao Y S., Gokulan R and Aravindan A. (2022). Investigation of Copper Ion adsorption using Activated Sawdust Powder: Isotherm, Kinetic and Thermodynamic studies, *Global NEST Journal*.

Jankowska k., Su Z., Zdarta J., Jesionowski T and Pinelo M. (2022). Synergistic action of laccase treatment and membrane filtration during removal of azo dyes in an enzymatic membrane reactor upgraded with electrospun fibers, *Journal of hazardous materials*, **435**, 129071.

Jegan J., Praveen S., Kumar B M.., Pushpa T B and Gokulan R. (2021). Box–Behnken experimental design for the optimization of Basic Violet 03 dye removal by groundnut shell derived biochar, *Desalination and Water Treatment*, **209**, 379–391.

Jegan J., Praveen S., Pushpa T.B and Gokulan R. (2020). Biodecolorization of Basic Violet 3 using biochar derived from agricultural waste: Isotherm and Kinetics, *Journal of Bio based materials and Bioenergy*, **14**(3), 316–326.

Jegan J., Praveen S., Pushpa T.B and Gokulan R. (2020). Evaluation of the adsorption capacity of Cocos Nucifera shell derived biochar for basic dyes sequestration from aqueous solution, Energy Sources, Part A: *Recovery, Utilization, and Environmental Effects*.

Jegan J., Praveen S., Pushpa T.B and Gokulan R. (2020). Sorption kinetics and isotherm studies of cationic dyes by arachis hypogaea shell derived biochar as low-cost adsorbent, *Applied Ecology and Environmental Research*, **18**(1), 1925–1939.

Kalyani G., Gokulan R and Sujatha S. (2021). Biosorption of zinc metal ion in aqueous solution using biowaste of Pithophora cleveana wittrock and Mimusops elengi, *Desalination and Water Treatment*. **218**, 363–371.

Kalyani G., Mahendran S.P and Gokulan R. (2020). Removal of lead metal ion using biowaste of Pithophora cleveana wittrock and Mimusops elengi, Energy Source Part A: Recovery, *Utilization and Environmental Effects*.

Kumar M., Sujatha S., Gokulan R., Vijayakumar A., Praveen S and Elayaraja S. (2021). Prediction of RSM and ANN in the remediation of Remazol Brilliant Orange 3R using biochar derived from Ulva Lactuca, *Desalination and Water Treatment*, **211**, 304–318.

Kumar M.S., Sivasankar V and Gopalakrishna G.V.T. (2017). Quantification of benzene in groundwater sources and risk analysis in a popular South Indian Pilgrimage City–a GIS based approach, *Arabian Journal of Chemistry*, **10**, S2523–S2533.

Kumar V.S., Gokulan R., Geetha M.B and Rahman D.Z. (2022). Biosorption of heavy metal ions from the aqueous solutions using groundnut shell activated carbon: batch adsorption, kinetic and thermodynamic studies, *Global NEST Journal*.

Lach C., Pauli C., Coan A., Simionatto E and Koslowski D.A.L. (2022). Investigating the process of electrocoagulation in the removal of azo dye from synthetic textile effluents and the effects of acute toxicity on Daphnia magna test organisms, *Journal of water process engineering*, **45**, 102485.

Lo F.S., Wang Y.S., Tsai J.M and Lin D.L. (2012). Adsorption capacity and removal efficiency of heavy metal ions by Moso and Ma bamboo activated carbons, *Chemical engineering research and design*, **90**, 1397–1406.

Madhu K., Ravindiran G., Sivarethinamohan S., Pathanjali S.P.S., Saravanan P and Sellappan E. (2021). Biodecolorization of Reactive Red 120 in batch and packed bed column using biochar derived from Ulva reticulata, Biomass Conversion and Biorefinery.

Mahendran S., Gokulan R., Aravindan A., Rao H.J., Kalyani G., Praveen S., Pushpa T.B and Senthil Kumar M. (2021). Production of Ulva prolifera derived biochar and evaluation of adsorptive removal of Reactive Red 120: batch, isotherm,

kinetic, thermodynamic and regeneration studies, *Biomass Conversion and Biorefinery*.

Moradi O., Pudineh A and Sedaghat S. (2022). Synthesis and characterization Agar/GO/ZnO NPs nanocomposite for removal of methylene blue and methyl orange as azo dyes from food industrial effluents, *Food and chemical toxicology*, **169**, 113412.

Murugadoss R.J., Kalyani G., Gokulan R., Sivaprakasam P., Maheandera Prabu P., Aravindan A., Praveen S and Senthil Kumar M. (2021). Biochar from waste biomass as a biocatalyst for biodiesel production: an overview, *Applied Nanoscience*.

Praveen S., Gokulan R., Jegan J and Pushpa T.B. (2021). Techno-economic feasibility of biochar as biosorbent for basic dye sequestration, *Journal of Indian Chemical Society*.

Praveen S., Jegan J., Pushpa T B and Gokulan R. (2021). Artificial Neural Network Modelling for Biodecolorization of Basic Violet 03 from aqueous solution by biochar derived from agro-bio waste of groundnut hull: Kinetics and Thermodynamics, *Chemosphere*, Article ID.130191.

Praveen S., Jegan J., Pushpa T.B and Gokulan R. (2021). Evaluation of the adsorptive removal of cationic dyes by greening biochar derived from agricultural bio-waste of rice husk, *Biomass Conversion and Biorefinery*.

Praveen S., Jegan J., Pushpa.T.B., Gokulan R and Bulgariu L. (2022). Biochar for removal of dyes in contaminated water: an overview, *Biochar*, **4**, Article ID: 10, 1–16.

Priya A.K., Gokulan R., Vijay Kumar A and Praveen S. (2020). Biodecolorization of remazol dyes using biochar derived from Ulva reticulata: Isotherm, Kinetics, Desorption and Thermodynamic Studies, *Desalination and Water Treatment*, **200**, 286–295.

Pushpa T.B., Josephraj J., Saravanan P and Ravindran G. (2019). Biodecolorization of Basic Blue 41 using EM based Composts: Isotherm and Kinetics, Chemistry select, **4** (34), 10006–10012.

Pushpa T.B., Praveen S., Gokulan R and Jegan J. (2021). Continuous sorption of methylene blue dye from aqueous solution using effective microorganisms-based water hyacinth waste compost in a packed column, *Biomass Conversion and Biorefinery*.

Ragunath S., Atchyuth B.S.A., Rao S.G.V.R and Gokulan R. (2022). Biodecolorization of Remazol Black B using Biochar produced from Coconut Shell: Batch, Desorption, Isotherm and Kinetic Studies, *Global NEST Journal*.

Rajeshkumar V A., Senthil Kumar M., Al-Zaqri N and Boshaala A. (2023). Adsorption of cationic dye (Red 95) from aqueous solution by biosynthesized nano particle of cumnium cyminum, *Global Nest Journal*, **25**, 1–10.

Rao J.H., Gokulan R., Ragunath S and Praveen S. (2021). Optimization of process conditions using RSM and ANFIS for the removal of Remazol Brilliant Orange 3R in a packed bed column, *Journal of Indian Chemical Society*.

Ravindiran G. (2014). Best dilution ratio and GCMS analysis for the removal of nutrient from municipal wastewater by microalgae, *International Journal of Chemtech Research*, **06** (01), 663–672.

Ravindiran G. and Ragunath S. (2014). Comparative study on treatment of municipal wastewater with carbon dioxide sequestration by microalgae, *International Journal of ChemTech Research*, **06**(01), 609–618.

Ravindiran G., Elayaraja S., Navaneethan P., Rajeshkannan R and Abinaya S. (2014). Assessment of physicochemical characteristics of municipal wastewater by microalgae, *International Journal of ChemTech Research*, **06**(01), 515–520.

Ravindiran G., Ganapathy P.G., Josephraj J. and Alagumalai A. (2019). A Critical Insight into Biomass Derived Biosorbent for Bioremediation of Dyes, Chemistry select, 4(34), 9762–9775.

Ravindiran G., Jeyaraju M.R., Josephraj J. and Alagumalai A. (2019). Comparative Desorption Studies on Remediation of Remazol Dyes Using Biochar (Sorbent) Derived from GreenMarine Seaweeds, Chemistry Select, **4**(25), 7437–7445.

Ru J., Wang X., Wang F., Cui X., Du X and Lu X. (2021). UiO series of metal-organic frameworks composites as advanced sorbents for the removal of heavy metal ions: Synthesis, applications and adsorption mechanism, *Ecotoxicology and Environmental safety*, **208**, ID.111577.

Saravanan R.V., Yuvaraja R., Andal L and Gokulan R. (2022). Batch, thermodynamic, and regeneration studies of Reactive Blue 19 using Ulva reticulata (biochar), *Desalination and Water Treatment*, **267**, 231–239.

Senthil Kumar M., Kalyani G., Mahendran S., Rao J.H., Gokulan R., Someswaran R., Latha J.C and Palpandian M. (2021). Treatment of RO rejects wastewater by integrated coagulation cum adsorption process, *Polish Journal of Environmental Studies*, **30**, No. 5, 1–8.

Sujatha S., Gokulan R., Rao H.J., Kalyani G., Praveen S and Senthil Kumar M. (2021). Effective removal of remazol brillinat orange 3R using a biocharderived from Ulva reticulata, Energy Source Part A: Recovery, *Utilization and Environmental Effects*.

Sujatha S., Rao H.J., Kalyani G., Gokulan R and Avinash A. (2021). Toward sustainable biodiesel production by solar intensification of waste cooking oil and engine parameter assessment studies, *Science of The Total Environment*, **804**, Article ID.150236.

Sundar L.M., Kalyani G., Gokulan R., Ragunath S and Rao J.H. (2021). Comparative adsorptive removal of Reactive Red 120 using RSM and ANFIS models in batch and packed bed column, *Biomass Conversion and Biorefinery*.

Wang R., Deng L., Fan X., Li K., Lu H and Li W. (2021). Removal of heavy metal ion cobalt (II) from wastewater via adsorption method using microcrystalline cellulose–magnesium hydroxide, *International journal of biological macromolecules*, **189**, 607–617.

Zhu H., Chen S and Luo Y. (2023). Adsorption mechanisms of hydrogels for heavy metal and organic dyes removal: A short review, *Journal of Agriculture and food research*, **12**, ID.100552.